applied sciences

MDPI

Article

Using A Rotary Spring-Driven Gripper to Manipulate Objects of Diverse Sizes and Shapes

Safal Lama and Taher Deemyad *

Department of Mechanical Engineering, College of Science and Engineering, Idaho State University, Pocatello, ID 83209, USA; lamasafa@isu.edu

* Correspondence: taherdeemyad@isu.edu; Tel.: +1-(208)-282-5655

Abstract: This paper introduces a new gripper mechanism that is capable of grasping objects of various sizes and shapes without the need for a closed-loop control system. Industries such as the food and beverage industry are seeking innovative soft grippers with a simplified control system. The proposed design utilizes a rotary mechanism with springs to achieve both force-closure and form-closure grasping. The design sets itself apart from most soft grippers with its ability to offer grasping forces in all lateral directions. The gripper is designed in a cylindrical shape and is actuated by a stepper motor with a gearbox to enhance the torque. Three stacked curvilinear and linear rails convert the motor's rotational motion into linear motion. The grasping component consists of three curved parts, each incorporating numerous compression springs. Currently, the gripper can effectively grasp objects ranging from five to nine centimeters in diameter, with a maximum height of ten centimeters. However, the design is scalable based on specific application requirements. A comprehensive CAD model of the mechanism was developed, and multiple analyses were conducted, including motion, topology, and stress analyses. Finally, a functional prototype of the gripper was constructed and successfully tested for grasping fruits and vegetables of different sizes and shapes. This research can be further expanded to explore the application of the gripper in space exploration with its novel and completely electro-mechanical foundation.

Keywords: novel grasping; spring-based system; open-loop control; minimum actuation; soft grasping; rotary system; pin array design; prototype; packaging system

Citation: Lama, S.; Deemyad, T. Using A Rotary Spring-Driven Gripper to Manipulate Objects of Diverse Sizes and Shapes. *Appl. Sci.* **2023**, *13*, 8444. https://doi.org/10.3390/app13148444

Academic Editors: Dimitris Mourtzis, Ossama Mokhiamar, Semaan Elias Amine, Haitham El-Hussieny and Khaled Elgeneidy

Received: 17 June 2023
Revised: 8 July 2023
Accepted: 18 July 2023
Published: 21 July 2023

1. Introduction

The world is currently experiencing the robotics revolution, marking a significant milestone after almost a century of industrial and manufacturing advancements [1]. Automation and robotic systems have permeated various aspects of human lives, holding the potential to revolutionize employment and organizations [2]. Military robots, which were once confined to the realm of science fiction, have now become a tangible reality [3]. Additionally, robotic manipulators have emerged as invaluable tools across diverse applications, capturing the attention of scientists and researchers [4].

The rapid expansion of the global population has created an escalating demand for food and beverages, prompting companies to transition from traditional packaging systems to automation and robotics. However, while these endeavors emphasize technological sophistication, simplicity in design is often overlooked. Moreover, the high initial cost and maintenance expenses associated with robotic systems render them impractical for small-scale and local companies. As a result, companies prioritize specific parameters when considering automation solutions, including multitasking capabilities, simplicity in part interchangeability, and cost-effective part replacement.

Within the human body, hands hold paramount importance due to their primary function of grasping objects. In 2000, the Utah/MIT dexterous hand stood out as one of the most sophisticated multi-fingered robotic hands developed to date [5]. Despite significant

technological advancements, most grippers still imitate the capabilities of human hands, primarily serving as platforms for testing and developing tactile sensing systems [6]. Experimental studies have unveiled the following three unique manipulative abilities that are exclusive to humans: precise handling, forceful precision grasping, and power squeezing [7]. These abilities encompass a wide range of human activities that have fostered safety, prosperity, and luxury in human civilization.

Technological push, encompassing mechanization, automation, digitalization, networking, and miniaturization have become integral parts of the industrial practice [8]. This demand has led to groundbreaking inventions aimed at reducing repetitive actions and enhancing consumer convenience. Affordable mass-produced motor vehicles have empowered millions of low-income consumers, while smart image processing has revolutionized product quality control. Robotic bartenders now serve drinks in bars, significantly impacting people's lives.

Robotic grippers play a vital role in enabling robots to execute repetitive tasks effectively. While some robots rely solely on mechanical functions, others integrate advanced features such as communication and feedback systems [9]. As end-of-arm tools, robotic grippers stand as indispensable components of robotic manipulators, distinguishing the overall process of robotic manipulation [9]. Their significance extends beyond industrial applications, and they have been used in fields like surgery, rehabilitation, and space exploration. This also can be understood more by studying the importance of industrial robots [10]. Vision-based robotic systems utilizing diagnostic images facilitate precision cutting, drilling, and other surgical tasks [11]. In the domain of rehabilitation, robotic grippers are instrumental in restoring manipulative functions for disabled individuals, bridging the gap between the user and the environment [11]. Furthermore, in space exploration missions, robotic grasping tools play a crucial role in remote sample collection. Researchers have explored various types of grippers, ranging from mechanical grippers to sensory feedback grippers, multiple-fingered grippers, vacuum grippers, adhesive grippers, clamp grippers, roller grippers, air hand grippers, and inchworm grippers, to achieve novel functionalities and address diverse application requirements [9].

The integration of machine learning techniques in vision-based grasping has opened new avenues for data-driven approaches, particularly in the realm of tactile sensing [12]. Also, tactile sensing stands to benefit greatly from machine learning, as demonstrated by designs such as the Utah/MIT multi-fingered robotic hand and other innovative solutions [13–16]. Furthermore, the design and fabrication of soft robotic grippers have garnered significant attention from researchers in recent years, owing to their lightweight nature, cost effectiveness, ease of fabrication, and control [17]. These grippers are actuated using pneumatic pressure, allowing for the flexible adjustment of pressure levels to accommodate different grasping tasks [17]. While most of the research is heavily focused on soft gripping materials and their structures [18–22], researchers have also proposed innovative mechanical gripper designs tailored for specific applications, such as capturing noncooperative satellites' aluminum honeycomb panels, drawing inspiration from ancient pole-/tree-climbing techniques, and so on [23–26]. In this research, a novel rotary pin array gripper [27] was designed and studied. This mechanism acts as a universal gripper with the ability to safely grasp a wide range of objects.

The overall flow of this paper begins with detailed information about the parts and mechanism of the design, followed by the analytical studies conducted to improve the design, and finally, the grasping test and validation.

2. Materials and Methods

2.1. Parts and Specification of the Mechanism

Traditional end-of-arm designs have historically drawn inspiration from the intricate structure and functionality of the human hand and fingers. The human hand comprises interconnected bones and muscles, which are coordinated through neuron signals. In the realm of kinematics, bones serve as linkages, muscles act as actuators, and nerves establish

connections to transmit voltage signals to control the motion. However, comprehending and creating a robotic hand with comparable capabilities is challenging. Designing such a robotic hand is more intricate than it may initially appear. As a result, soft and innovative grippers have emerged as viable alternatives, garnering significant interest in their potential to revolutionize hardware automation in recent years.

In this research, the proposed gripper comprises multiple components, as illustrated in Figure 1 and listed in Table 1. At the core of the mechanism are three shutter components (#5), which are three equal pieces of a cylindrical extrusion. The shutters contain small holes (cylinders) intended for the insertion of small pistons (#12) and springs (#13), which, together, function as flexible grippers. Also, each shutter contains a small column on the top and bottom faces. Half of the column on top has a rectangular extrusion, the other half has a cylindrical extrusion, and the bottom column only has a rectangular extrusion (Figure 2). These columns enable the shutter to slide inside the circular plates above and below.

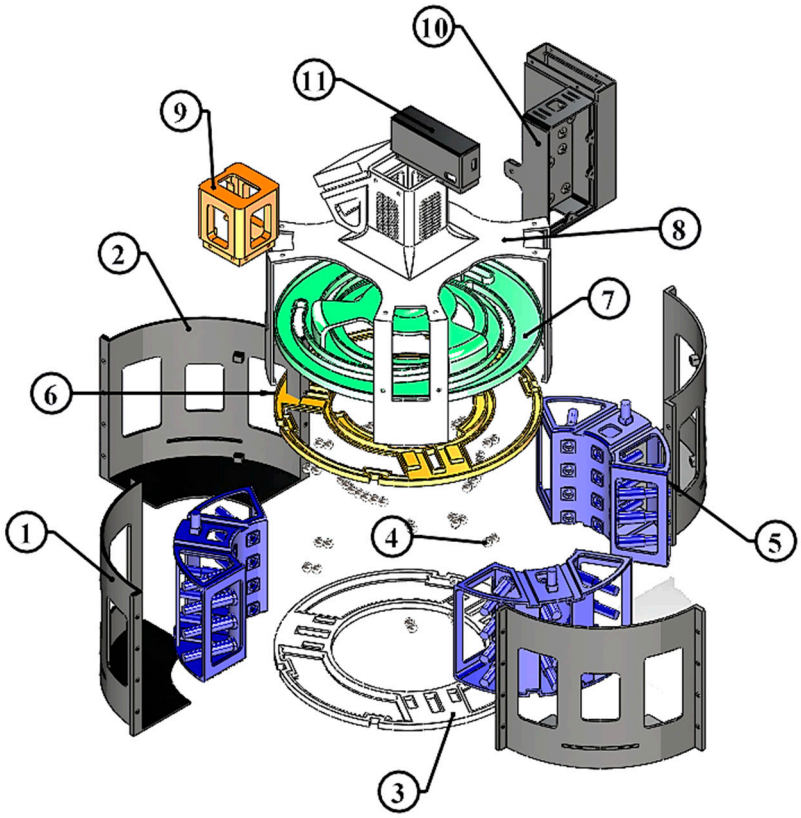

Figure 1. Exploded view of the design with balloon numbering as part numbers from Table 1.

Two types of circular plates are in the design. (a) Linear guide circular plates are located at the bottom (#3) and top (#6), featuring rectangular-shaped slots; these plates serve as guides for the shutters, ensuring they move in a straight path. (b) Curvilinear guide circular plates (#7) are situated on top of the linear guide circular plate at the top (#6). The curvilinear slot in this plate spans 120 degrees of arc, starting from the bottom of one linear cut and ending at the top of another linear cut in the linear guide plate (#6). The curvilinear slots transfer torque from the motor to the shutters. To minimize friction between the plates, grease lubricant is applied, and steel bearing balls (#4) are incorporated within the designed rails between the circular plates to ensure smoother motion. Similar rails, with bearing balls, are implemented between the shutter and linear guide plates (#3 and #6) to facilitate smooth motion. All the components are enclosed within the outer shells (#1 and #2), which are fastened together to form a box-like structure or outer cover, allowing for space at the bottom for the entry of the target object. The gripper's internal

components (#3, #5, #6, and #7) are secured together by screws from the top part (#8), which also houses the motor.

Table 1. Designed parts with dimensions and part numbers.

Part's Name	Dimensions (cm) [1]	Part No.
Outer Shell A	H = 14.7, OR = 14.3, T = 0.3	1
Outer Shell B	H = 14.7, R = 14.3, T = 0.3	2
Rectangular Slot Plate (Bottom)	OR = 13.9, IR = 8, T = 0.75	3
Bearing Ball	D = 1	4
Shutter	OR = 11, IR = 5, H = 15.25	5
Linear Slot Plate (Top)	OR = 13.9, IR = 6.8, T = 0.75	6
Curvilinear Slot Plate	OR = 13.9, IR = 6.8, H = 5.4	7
Top Cover	OR = 14.8, H = 24.6	8
Motor Cover	6.3 × 6.3 × 7.8	9
Electronics Box	10.2 × 10.275 × 14.7	10
Wire Cap	10.2 × 3.075 × 5.19	11
Piston	R = 0.15, H = 6	12
Spring	R = 0.5, T = 0.05, H = 2.5	13
Piston Blocker	OR = 0.6, IR = 0.25, H = 0.4	14

[1] Only important dimensions are shown; in the dimension column, O = outer, I = inner, R = radius, T = thickness, and H = height.

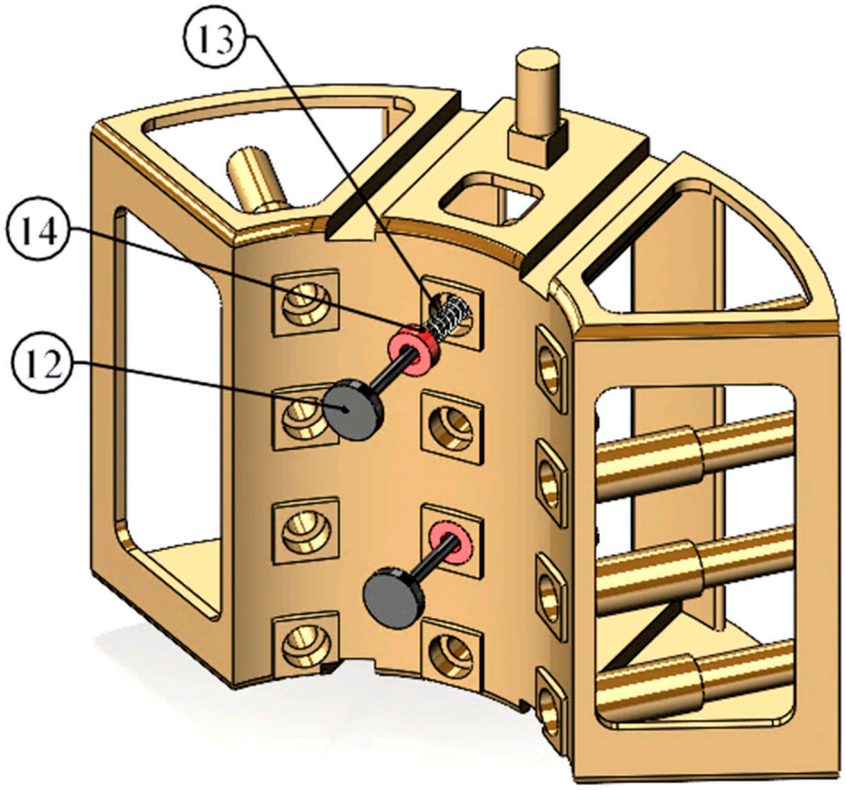

Figure 2. Shutter CAD model with balloon numbering as part numbers from Table 1.

The motion from the motor's rotation is transmitted to the curvilinear guide circular plate (#7) through a shaft hole and key. This rotational motion is then transferred to the shutters, which can only follow the linear path defined by the linear guide circular plates,

converting the motor's rotational motion into linear motion. The grasping state is achieved when the shutters come into contact and form a circular shape.

During the design-to-assembly (DFM) process, meticulous attention is given to each part to ensure precise assembly and optimal performance. Carefully determined dimensions facilitate easy assembly and enable the gripper to effectively grasp objects with diameters of 5 cm to 9 cm, encompassing typical vegetables and fruits in grocery stores. However, this design is fully scalable to manipulate objects of different sizes based on user requirements and specific applications. The gripper's diameter can be adjusted to accommodate objects within different size ranges. Additionally, the springs can be readily replaced with alternative springs possessing distinct spring constants, thereby allowing for gripper customization based on the objects' texture (e.g., soft or fragile items) or maximum weight.

In the current prototype, the overall assembly has a radius of approximately 14.3 cm, which corresponds to the radius of the outer shells (#1 and #2). The design's total height measures around 34.15 cm (excluding the wire cap), with the top part (#8) housing the motor and gearbox, adding to its height. The top part is rigidly connected to the outer shells. The motor, which is housed within the top cover part, imparts rotational motion, generating circular movement of the curvilinear guide plate (#7), which features a 120-degree slot mechanism that drives the top column of the shutter (#5). All circular plates have an outer diameter of 27.8 cm and a thickness of 0.75 cm. The shutters have outer and inner diameters of 22 cm and 10 cm, respectively, along with a height of 15.25 cm.

Figure 2 depicts an image of the shutter with a column extending from its top face. This column maintains contact with the following two distinct plates: the linear guide circular plate (#6) and the curvilinear guide circular plate (#7). The linear guide plate incorporates a slider connection with 1 degree of freedom (DOF), while the curvilinear guide plate features a roller connection with 2 DOFs. A hidden rectangular extrusion is present on the bottom face, serving a similar function as the one on the top face. The motion is initiated when the motor rotates the curvilinear guide plate (#7), causing the circular column to follow the path defined by the slot. The linear guide plate (#6) constrains the motion, resulting in the linear movement of the shutter. The outer face of the shutter contains 12 precisely designed holes, intended for the integration of springs and pistons to provide grasping force. The springs are allowed to fully deflect, with a length of 2.5 cm. The pistons are equipped with sticky material at the contact tip to enhance grasping performance, and are made of M3 screws, with a height of 6 cm. Figure 2 depicts the exploded view of one of the shutters and the components inside of it. Each shutter includes the pistons, spring, and piston blocker. This figure shows the assembling process of the pistons (top) and an assembled piston (bottom). In the final design, all holes are equipped with parts #12, #13, and #14.

2.1.1. Mechanical Advantage

This mechanism is based on a kinematic concept that incorporates compression springs and a piston arrangement within moving shutters for object manipulation. What sets this design apart from other spring-based grippers is its ability to achieve both force-closure grasping and form-closure grasping simultaneously, ensuring enhanced safety during grasping operations. Again, the grasping forces from all lateral directions on the object are something this gripper design offers, while most of the spring or pneumatic grippers are two-fingered. This design offers scalability through the flexibility to interchange the compression springs with varying spring constants. The application of Hooke's law along with the soft finger forces allows for each piston to calculate the force exerted on the grasped object's surface, considering the respective spring constant. Additionally, the application of rough material on the grasping tip of the piston head enhances the friction between the object and the pistons, resulting in a more efficient grasping performance. Throughout the design process, stress analysis, motion analysis, and topology optimization were employed to refine the mechanism, resulting in a final design that prioritizes lightweight construction, reliability, and optimal grasping performance.

2.1.2. Material Selection

The grasping mechanisms are very vulnerable to external factors. Therefore, proper material selection for the prototype of this mechanism, which faces various phenomena such as bending, friction, and uneven force distribution, is critical. Based on that, acrylonitrile butadiene styrene (ABS) plastic, because of its specific property, was considered for most parts of the prototype. ABS plastic filament is mostly used in 3D printing, and it is one of the strongest among other materials that are light in weight. This material is more feasible for this design in terms of the geometric structure that the machine must print. It also has sufficient tensile strength and can be printed with high precision. It can be sanded to desired smoothness without deformation, unlike some polylactic acid (PLA) plastics that tend to melt down during machine sanding. While the whole design is printed with ABS plastic, the pistons are made of steel. They are off-the-market screws that are stiff and perfect for the size requirement.

The total weight of the gripper and its actuation system is crucial with regard to the maximum payload of the robotic arm it is attached to. As the prototype of the design is made of ABS plastic, the weight-to-strength ratio remains decent for the design. Also, using ABS plastic provides quick prototyping abilities with decent remodeling and 3D printing. However, plastic parts bring frictional factors to their peak compared to fine-surface machine parts. Also, the use of plastic restricts the possibility of making it compact, leaving the prototype big and less appealing. The total weight of the system without the control/electronics system is 3.1 kg.

For the industrial version of this product, among all alternative materials with a higher stress tolerance and lower friction coefficient, 6061 aluminum alloy can be the most appropriate option based on similar research and material data presented in [28]. The final choice of material is made to be 6061 aluminum alloy, but only for high friction-prone parts, so that the overall weight of the system remains pretty much unchanged. Some of the specifications for these three materials are shown in Table 2.

Table 2. Material properties comparison.

Properties	6061 Aluminum Alloy	ABS
Yield Strength	276 MPa	29.6 MPa
Ultimate Tensile Strength	310 MPa	40 MPa
Elastic Modulus	69,000 MPa	2000 MPa
Poisson's Ratio	0.33	0.394
Mass Density	2700 kg/m^3	1020 kg/m^3
Shear Modulus	26,000 MPa	318.9 MPa

2.1.3. Electrical Component

The design presented in this paper consists of some general mechatronic components. These components are listed in Table 3.

The main electrical component used in most mechatronic projects is microcontrollers. An Arduino Uno R3 (#1), because of its proper size and because it has enough pins for all electrical components, was selected for this system. This microcontroller has 14 digital and 6 analog pins with multiple grounds. It also consists of voltage output pins that can be used for powering different components such as sensors, buttons, motors, and so on. As depicted in Figure 3, Arduino Uno R3 is connected to all components. It is programmed to incorporate the remote control that communicates via the HX1838 remote (#4) and the VS1838 NEC Infrared Wireless sensor module (#5). The sensor module is connected to Arduino to its digital pin 2, 3.3 V pin, and the ground. It is programmed to control the clockwise and anticlockwise rotation of the PKP Series 2-Phase Stepper Motor (#3).

Table 3. Electronic components referring to Figure 3.

Electrical Components	Quantity	Component No.
Arduino Uno R3	1	1
L298N Motor Driver Module	1	2
PKP Series 2-Phase Stepper Motor	1	3
Remote Control Module	1	4
HX1838 VS1838 NEC IR Receiver	1	5
6 mm × 6 mm × 5 mm Tactile Push Button	3	6
10 kΩ Resistor	3	7

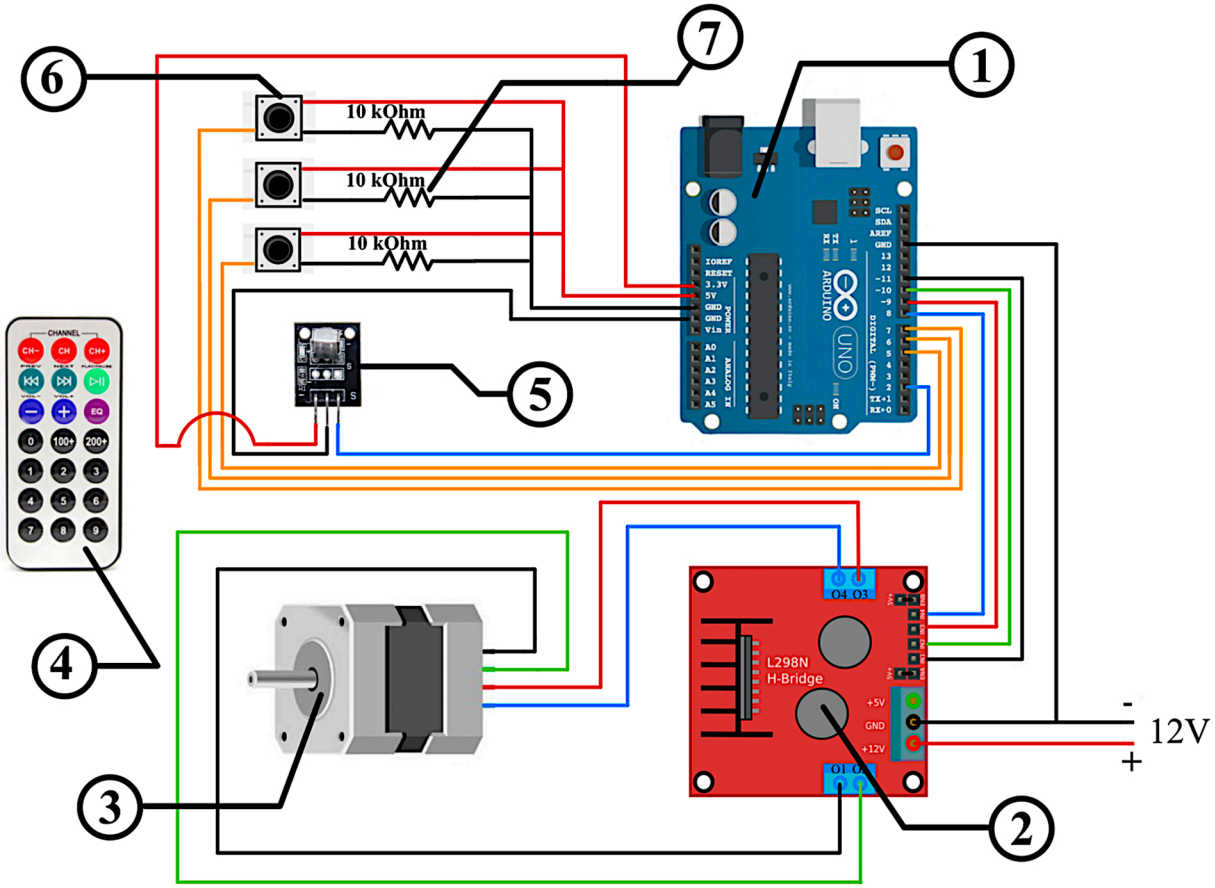

Figure 3. Electric circuit diagram with balloon numbering as the part number from Table 3.

The motor is connected to the Arduino Uno R3 via the L298N Motor Driver Module (#2). The four wires coming out of the motor are identified with their colors using the description of the motor in [29]. They are connected as shown in Figure 3. Pin1, Pin2, Pin3, and Pin4 are connected to the Out1, Out2, Out3, and Out4 of the L298N module, respectively. Further, the four wires from the L298N Driver, IN1, IN2, IN3, and IN4 are connected to the four digital pins 8, 9, 10, and 11, respectively, of the Arduino board for control purposes. The motor and the controller are powered using an external power source as shown. For safety and error minimization, 3 push buttons (#6) are used to bring the program to a stop. These buttons are placed to stop motion at its extreme positions. This helps the system to eliminate the step motion error in the motor over the long run and motor and parts damage. These push buttons are connected to a digital pin, 5 V pin, and GND of Arduino with 10 kΩ resistors (#7) in grounding.

2.2. Kinematic Analysis

The side view of the moving parts in the proposed mechanism is shown in Figure 4. The motion begins with the curvilinear slot plate (Part A), which is rotated by the motor. The curvilinear slot plate drags the shutter (Part C), which is guided toward the direction of the motion by the rectangular slot plate (Part B). Because the force from the motor only applies to the top part of the mechanism, the friction creates a bending moment within the parts and causes problems in the smooth motion of the shutters. This problem was almost solved by minimizing the friction between parts using the motion slots with bearing balls greased with NLGI Grade 2 Lithium Grease.

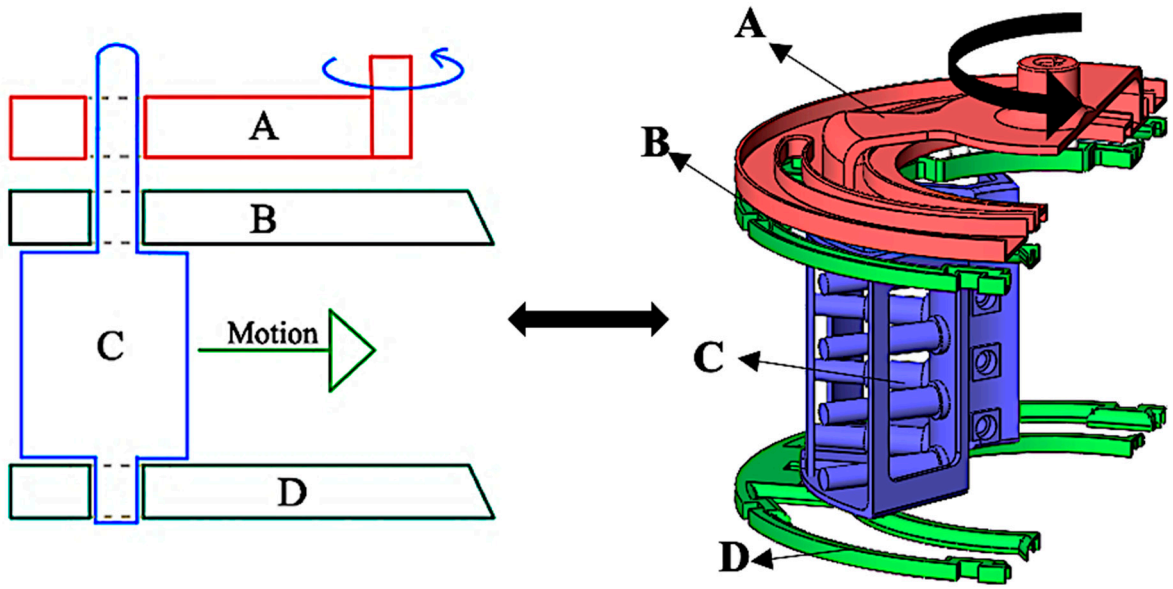

Figure 4. General study of dynamics with parts denoted as A, B, C, & D (side views).

The mobility of a mechanism refers to its number of independent degrees of freedom, which determines the number of required actuators. The mobility of a mechanism can be determined using Equation (1) (Chebychev–Grübler–Kutzbach equation) for a planar motion. Over-constrained mechanisms with zero or negative mobility are considered structures, and they cannot create any motion. However, some exceptional cases with negative mobility are still movable based on their particular geometry (e.g., Bennett linkage [30]). In the current mechanism, based on the geometry of its axes of motion, mobility can be considered in the subgroup of motion and can be analyzed as a planar motion.

$$M = 3(n-1) - \left[\sum_{i=1}^{j} (3 - f_i),\right] \quad (1)$$

where n is the number of links, j is the number of joints, and f_i is the degree of freedom for each type of joint.

Figure 5 illustrates the kinematic sketch of the mechanism, providing a clearer understanding of the motion. Although the kinematic sketch is not drawn to scale, it accurately demonstrates the intended motion of the proposed mechanism. Within this sketch, the ground link is denoted as L1, the curvilinear slot plate (#7) is denoted as L2, the shutter (#5) is denoted as L3, and the slider (#6) is grounded. The mechanism comprises the following three joints: J1, which is revolute; J2, a roller; and J3, a slider. J1 and J3 each possess one degree of freedom, while J2 possesses two degrees of freedom. By considering the number of joints, links, and degrees of freedom for each joint and applying them in Equation (1), the mobility of the machine can be determined as one, as indicated by Equation (2). Conse-

quently, this mechanism requires only one actuator to generate motion, which is ideal in terms of minimizing the number of actuators required and the weight of the mechanism.

$$M = [3(3-1)] - [2(3-1) + 1(3-2)] = 1 \quad (2)$$

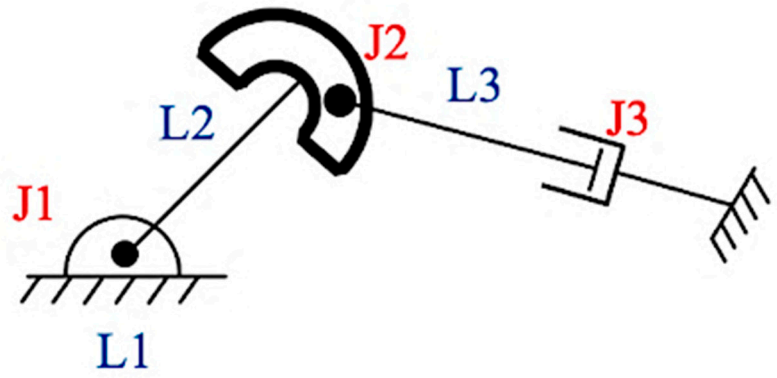

Figure 5. Kinematic sketch of the mechanism.

2.3. Force Analysis

The design is based on computer analysis, and the forces involved are divided into the following two main forces: the force from the actuator and the springs force. The force from the actuator makes the motion of the shutter mechanisms. The applied torque is calculated using the motor torque curve shown in Figure 6.

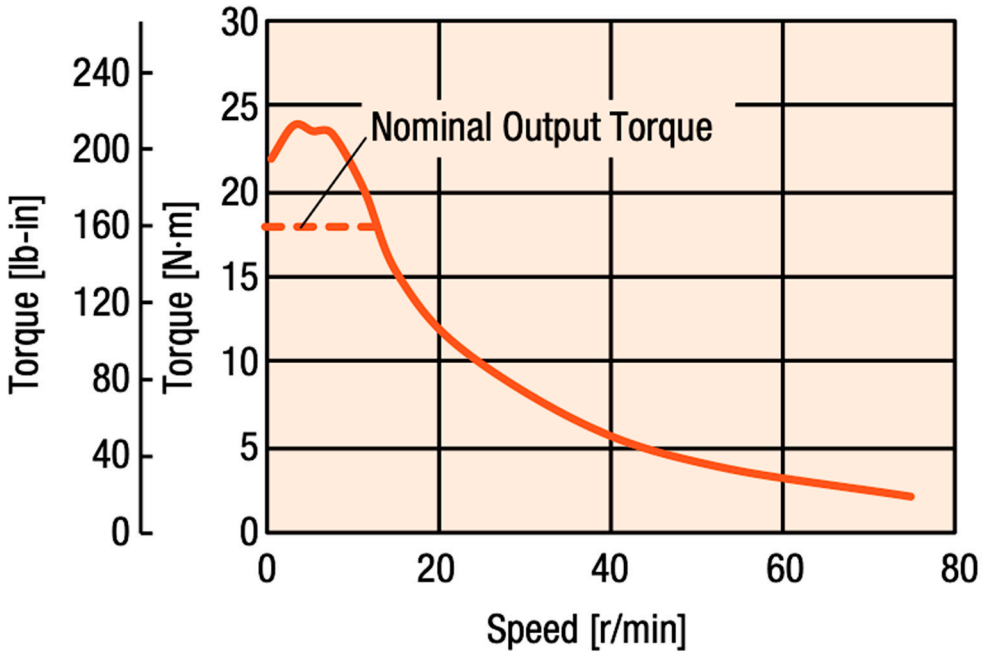

Figure 6. Speed (rpm) vs. torque (N-mm) chart for the motor.

Based on the relation between the torque and speed of the motor in Figure 6 and to obtain the maximum torque, this motor is programmed to rotate at a speed of 0–20 rpm. With the maximum deviation angle of θ = 38.05° from the tangential torque at a 9.5 cm radius, the normal force being applied is calculated using the free body diagram in the planar condition, as depicted in Figure 7.

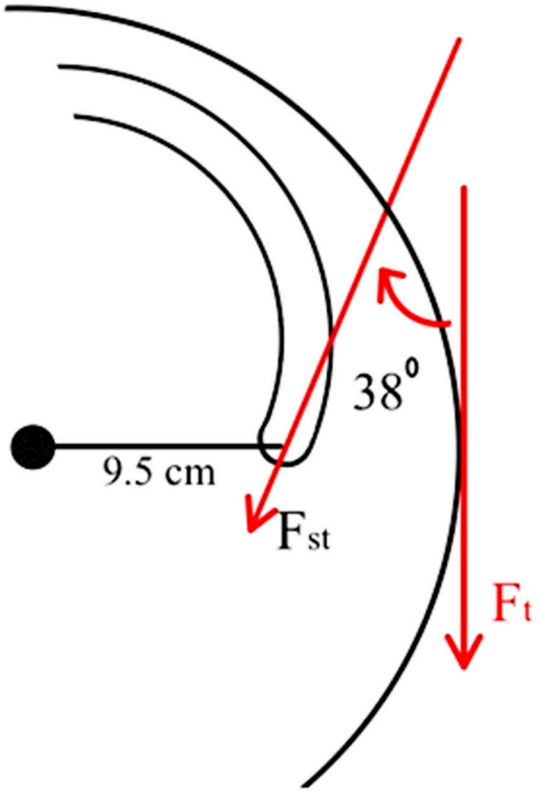

Figure 7. The tangential angle between the curve path and motor rotation path.

The tangential force (F_t) is calculated using Equation (3), where force is the only unknown term.

$$Torque\ (\tau) = F_t \cdot radius\ (r), \tag{3}$$

Using Equation (3) and referring to the free body diagram presented in Figure 7, the tangential forces acting on the slot curve, denoted as (F_{St}), are computed according to Equation (4). These tangential forces serve as the driving force for the actuation of the mechanism. It is important to emphasize that the centers of rotation and the curve path are different from each other.

$$F_t = F_{St} \cdot \cos(\theta), \tag{4}$$

Another significant force in this mechanism is the grasping force, generated through the compression of the springs. From Equation (5), the force exerted by a spring is influenced by the following two factors: displacement (x) and the spring constant (k). The spring constant is determined by the spring's dimensions (length, thickness) and its material properties. Moreover, the size of the object being grasped affects the displacement of the spring, with larger-diameter objects experiencing greater forces.

$$F_{spring} = -k \cdot x, \tag{5}$$

This spring-based grasping mechanism proves to be highly effective for grasping objects with varying diameters and shapes, if all objects possess a similar texture (i.e., soft or hard) and if the proper springs are selected. Furthermore, the interaction between the target object and the contact fingers (in this case, the pistons) significantly influences the grasping force.

Like other mechanical designs, the components within this mechanism possess a specific lifetime and require replacement after a certain period to maintain a reliable grasping system. The incorporation of springs in this mechanism provides the gripper with

the unique capability of grasping diverse objects. However, the properties of the springs gradually diminish over time, necessitating their replacement.

Performing a grasping analysis is necessary for any robotic gripper. This study was performed on this mechanism to ensure whether the object is being grasped properly and whether it is stable and safe inside of the gripper when the robotic manipulator has moved around. The mechanism presented in this paper includes force-closure grasping with soft fingers. However, because it uses several fingers all around the object, it can be considered as a form-closure gripper, too. A complete grasping of the object depends upon the following three main factors: numbers and positions of the fingers, types of fingers, and geometry of the object. This can be expressed via Equation (6).

$$\left\{ \sum_{i=1}^{k} n_i N_i, \quad n_i \in \mathbb{R} \right\} = Force \tag{6}$$

where 'n' is the normal force with respect to different axes, 'N' is the wrench space, and 'i' is the number of fingers.

The soft fingers provide optimal grasping with a force that is normal to the surface (F_{spring} in this case), frictional forces in the tangent plane, and the frictional moment in the normal direction, resulting in a 4-dimensional wrench subspace, as presented in Figure 8 and Equation (7). Not to mention, the soft finger forces depend more or less on the properties of the material on the piston tip.

$$F_w = \begin{Bmatrix} F_x & 0 \\ F_y & 0 \\ F_z & M_z \end{Bmatrix}, \tag{7}$$

In the equation above, F_x, F_y, and F_z represent the normal forces caused by friction between contact surfaces in the x, y, and z directions. Additionally, M_z is the constraining moment in the z-axis. Normal forces restrain movement in specific directions, while the moment prevents undesired rotation around the contact point. This ensures that the object being grasped will not slip or change orientation, allowing for a secure grip.

2.4. Stress Analysis

The design process of the proposed mechanism involved iterative simulations within a CAD software environment to obtain an optimized design. Most components underwent validation through finite element analysis (FEA) to ensure they met the criteria for maximum allowable deformation. Due to the intended attachment of the gripper to a high-speed industrial robotic arm (with speeds of up to 8000 mm/s), a high factor of safety was selected to prevent failures and ensure safety in the working environment. However, certain parts, such as the boxes for electrical components and the actuation system, were designed without stress analysis, as they were not subjected to significant forces. Also, during the stress analysis of various components, it was observed that the top part (#8) experienced the highest stress compared to the others, which is attributable to factors such as bearing the weight of the entire mechanism and employing minimal thickness for this part.

Furthermore, to minimize the total weight of the mechanism, a topology study was conducted to identify areas of each part where material could be removed while maintaining the same stress and load capacities. The studies were performed while considering a maximum load of 45 N, which is 1.5 times the maximum payload of the robotic arm. The results of the topology study were then used to refine and validate the design through FEA. As shown in Figure 9b, topology creates a picture determining the excess material that is safe to remove without compromising the structural strength. Similarly, the FEA in Figure 9a shows the possible displacement in the part due to load. The maximum displacement seemed to be just over 1.3 mm, which is very little and acceptable considering the location of it.

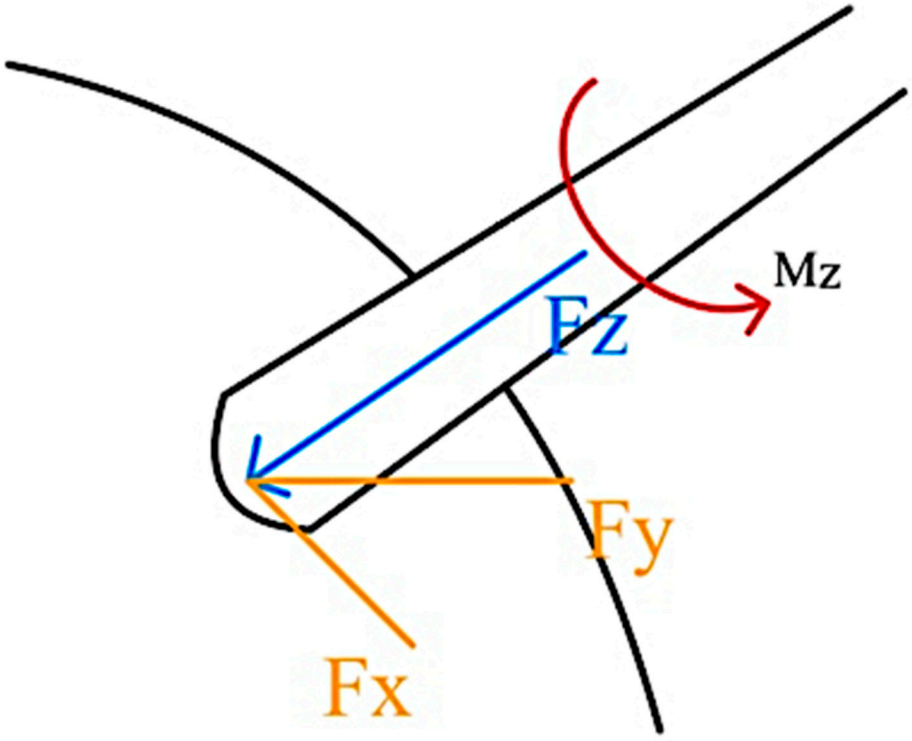

Figure 8. Soft finger and its forces.

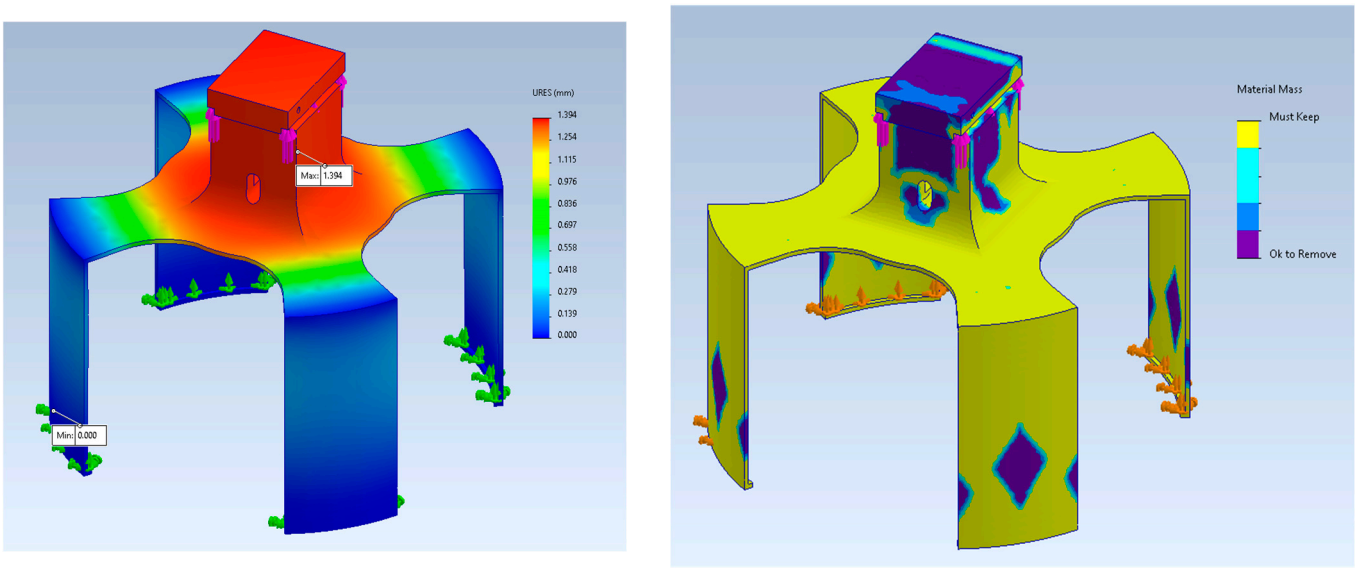

(**a**) (**b**)

Figure 9. (**a**) FEA displacement analysis for the top part; (**b**) topology study for the top part.

The design process involved creating, analyzing, and improving the design using FEA and topology studies. The outcomes of these studies for the top part (#8) are presented in Figures 9 and 10.

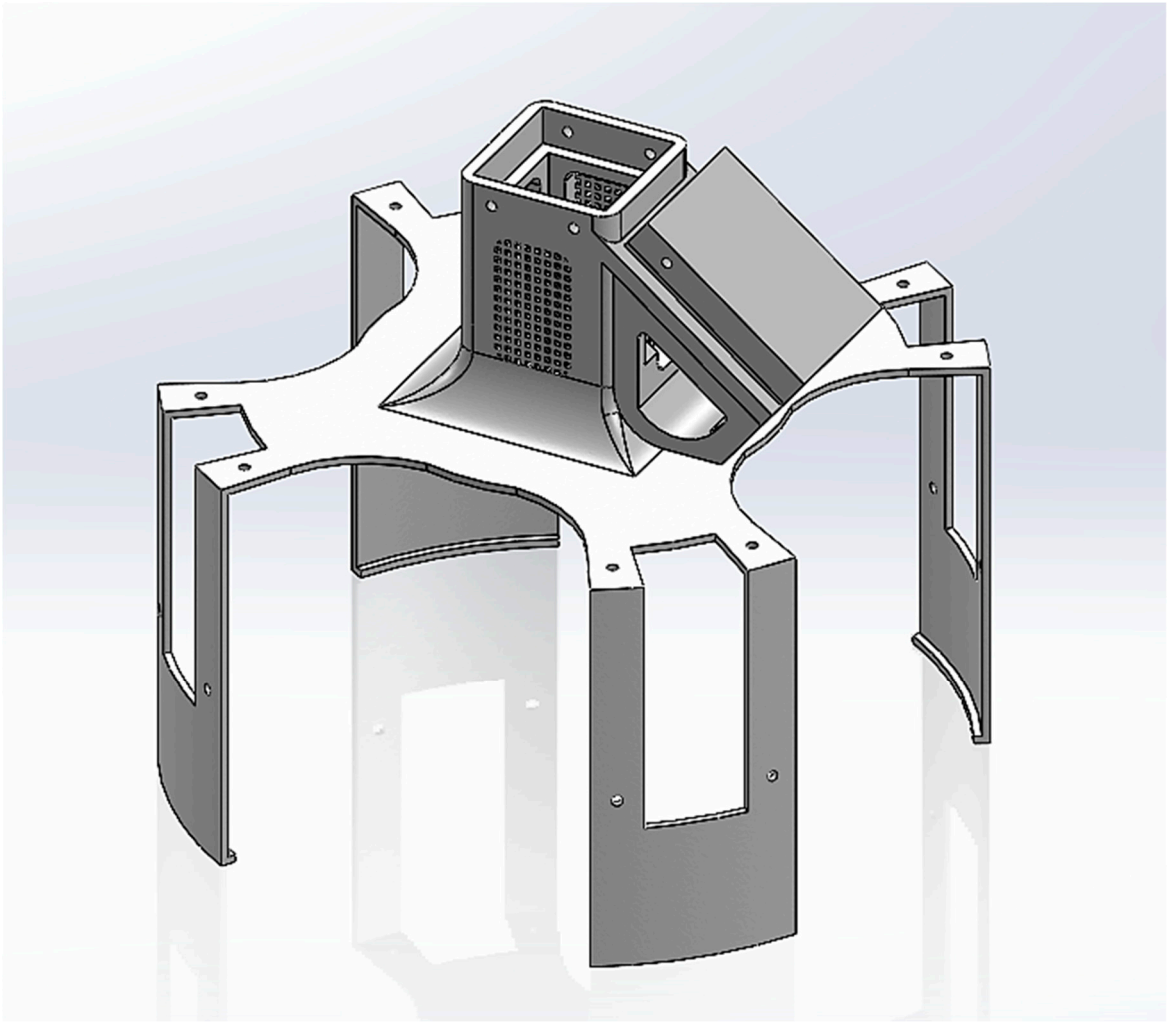

Figure 10. Improved top part considering analytical studies.

3. Results

The prototype of the proposed mechanism was constructed using additive manufacturing technology and fabricated using ABS plastic material. In addition to the essential components required for proper motion and object grasping, a dedicated control box (#10 and #11) was designed to house the controller, motor driver, and battery, which powers the actuation system. The control box is designed to protect all electronic components against potential contact with liquids that are present in the working environment. Moreover, by keeping the wires inside of this box, the gripper remains protected from wire entanglement with external objects, particularly during the high-speed movements of the robot. This design approach ensures a compact and integrated structure for the gripper as a whole, enhancing its functionality and safety.

The grasping test is performed by grasping various-sized and shaped objects in order to validate the design. The gripper has the following two major working stages: closing to grasp and opening to release.

As the motor receives a command via the IR receiver, the motor rotates to close the shutters so that the pistons with springs are pressed in by the target object, and the reaction force from the springs causes the object to be grasped.

To release the object at its destination, a reverse motion of the motor is employed, causing the shutters to move apart from each other. As a result, the springs return to their resting positions without any contact or interaction with the target object, leading to the release of the object from the gripper's grasp.

The final CAD model of the gripper, excluding the electronic components, is illustrated in Figure 11a. Furthermore, the physical prototype of the gripper is showcased in Figure 11b.

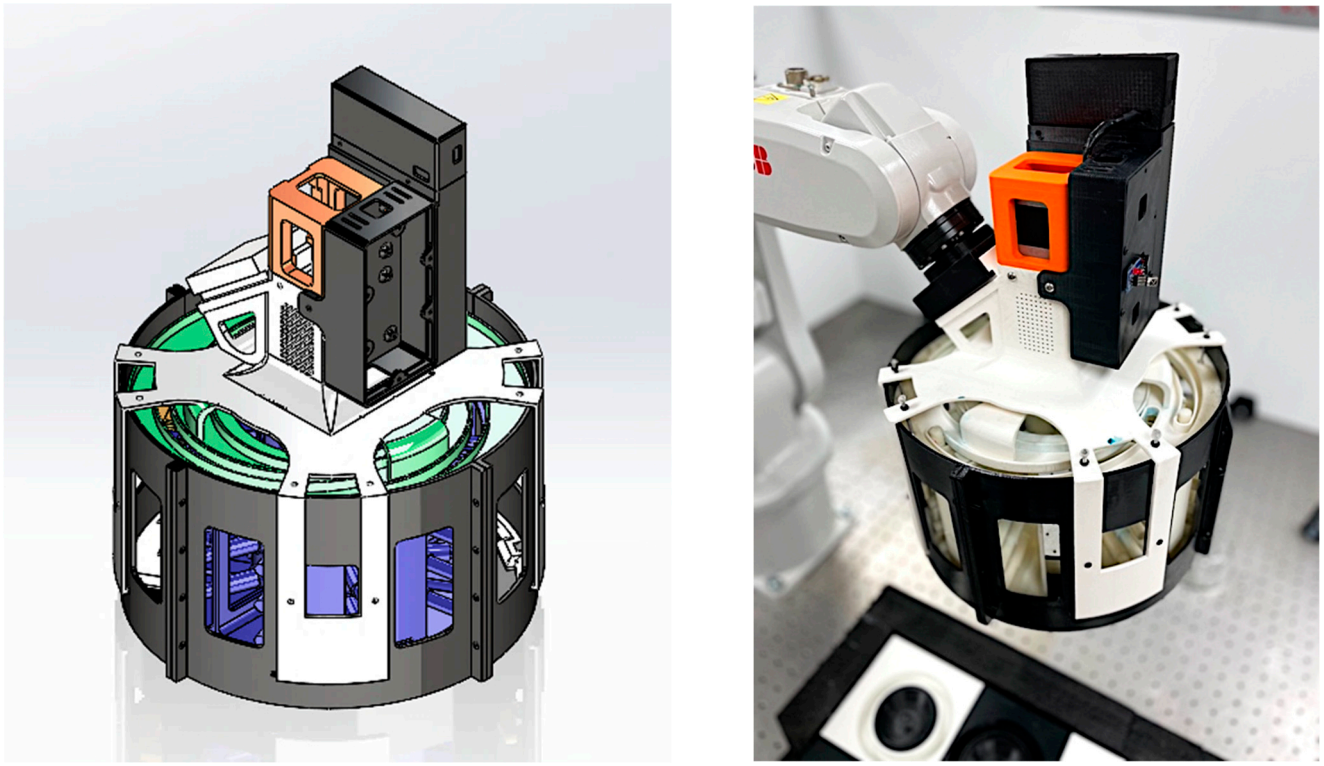

(**a**) (**b**)

Figure 11. (**a**) Design assembly excluding electronics, screws, and actuation system; (**b**) actual prototype attached to the 6-axis industrial robotic arm.

3.1. Motion Study

Motion analysis was conducted under the following two distinct conditions: one where the vertical motion of the top rotating plate was constrained, and another where it was not. It was observed that the absence of constraint on the vertical motion led to the unintended vertical movement of the top plates. This occurrence was attributed to imbalanced moments experienced by the shutter components, as illustrated in Figure 12. The issue arose because the actuation force was solely applied to the top part, resulting in a moment being exerted on a point located in the lower section of the shutter. Therefore, it is necessary to restrict the vertical movement of the top plate to preserve the smooth motion of the shutter within the designated plane.

Once the initial design phase is concluded, a motion analysis is conducted to assess the ability of the design to achieve the desired range of motion and to identify any necessary modifications. Additionally, a motion analysis is employed to calculate the torque that is necessary to accomplish the intended motion. Given the constraints of simulating real-world conditions, the motion study simulation is performed using available aluminum contact settings. The torque required to rotate the mechanism and execute the desired action is depicted in the chart presented in Figure 13.

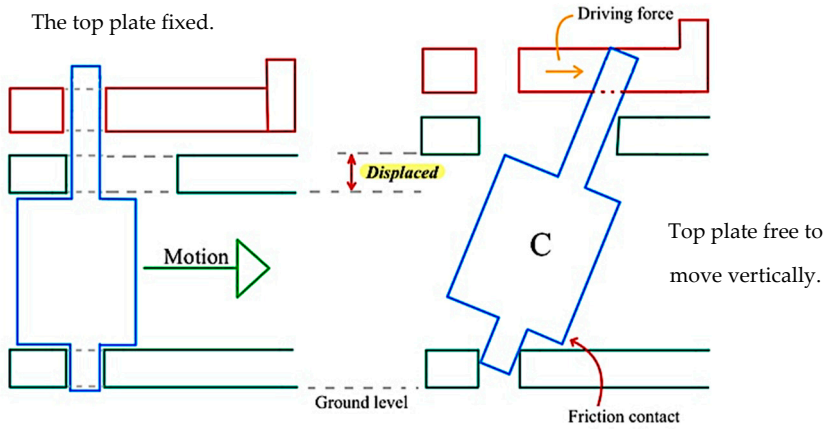

Figure 12. Visual representation of the motion study for non-constrained vertical motion of the curved plate.

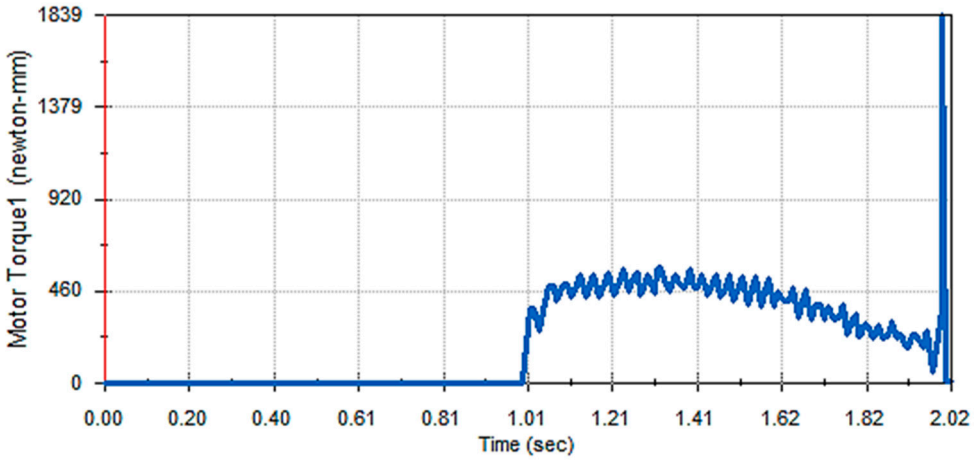

Figure 13. Motion study results for the torque required to actuate the system.

The torque analysis chart indicates that a maximum torque of approximately 575 N mm is required to achieve the desired motion. Various existing frictional factors contribute to significant resistance, leading to the high torque requirement. The observed torque increase towards the end of the chart occurs when the system reaches a point where further movement is not possible.

In this study, a 3D-printed ABS plastic prototype was utilized, which inherently lacks smooth textured surfaces. Despite attempts to enhance smoothness through sanding, achieving the required level of smoothness with a high precision proved to be challenging. Therefore, surface sanding, the implementation of NGLI Grade 2 Grease, and the incorporation of ball bearings between the adjacent surfaces were employed as methods to minimize friction to the greatest extent possible. Additionally, a motor with a 40:1 gear ratio was employed to generate sufficient torque for accomplishing the desired motion.

3.2. Robotic Arm Path Planning for Efficient Task Execution

The initial stage of achieving successful grasping involves ensuring that the gripper possesses the capability to reach the intended target object. Consequently, the use of a manipulation system becomes essential for executing the grasping action and subsequently transporting the object across diverse locations. Additionally, to facilitate the gripper's movement between task points, it becomes imperative to analyze the robot's kinematics and devise an appropriate path plan for the end effector. For this specific project, a small-

scale industrial robot, ABB IRB 120, was selected as the manipulation system based on the project's requirements.

In many cases, grasping operations are performed as part of a series of pick-and-place actions. To accomplish this, the robotic arm needs to be programmed to move and reach various target points. However, the robots can have limitations in reaching the target points due to the loss of one or more degrees of freedom, which are referred to as singularities in robotics.

Singularity occurs when the robot's tip becomes unable to move or generate velocities in specific directions. This condition is determined by evaluating the Jacobian matrix, represented as $J_{(\theta)}$. In the case of a serial 6-DOF (degree of freedom) robot, singularity arises when the determinant of the Jacobian matrix becomes zero, as indicated by the condition Equation (8). It is important to know that the expression of the Jacobian matrix can be in either the world frame or the body frame, while the singularity configuration remains independent of the chosen reference frame.

$$\det\left(J_{s(\theta)}\right) = 0 \;\rightarrow\; rank\left(J_{s(\theta)}\right) < 6 \tag{8}$$

For a serial 6-DOF robotic arm, there are several cases or conditions of singularity, and this study focuses on the five most common cases explained below as well as depicted in Figure 14.

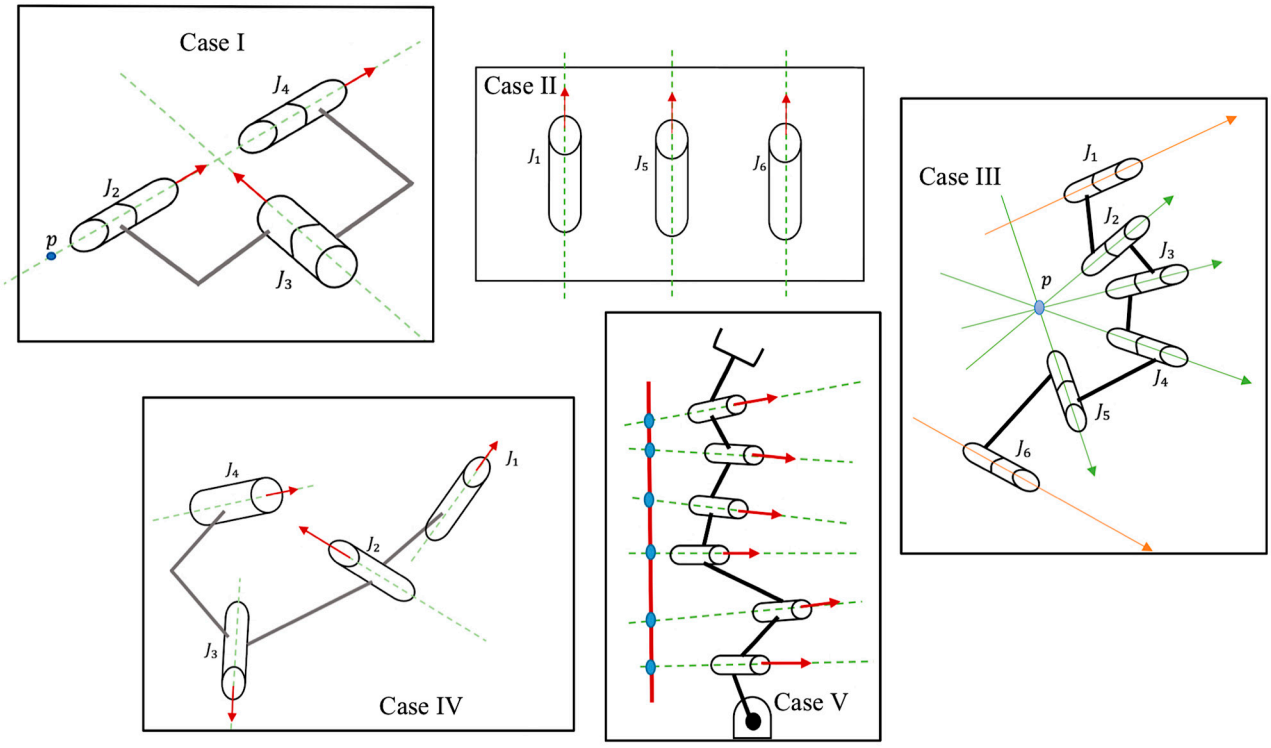

Figure 14. Five cases of singularity for a serial 6-DOF robotic manipulator.

Case I: Two collinear joints. In this case, when there are two joints with their z-axis in the same direction, the robotic end effector is unable to move at least in certain directions.
Case II: Three coplanar and parallel revolute joints.
Case III: Four revolute joints intersecting at a common point.
Case IV: Four coplanar revolute joints.
Case V: Six revolute joints intersecting the common line.

During the task definition process for testing the gripper with the robotic manipulator, careful consideration is given to ensure that none of the tasks fall into the singularity con-

figuration of the robotic arm. Additionally, to avoid encountering any singularity positions between consecutive tasks, an interpolation technique is employed, where 10 points are defined. The singularity of these points is assessed by calculating the determinant of the Jacobian matrix to verify that none of them equal zero. This analysis is conducted to identify any potential singular or near-singular conditions before the final testing phase.

The Jacobian matrices for all the joints and transformations of the ABB IRB 120 robot are already defined in [31]. Furthermore, a D-H parameter table is constructed based on the ABB IRB 120, as depicted in Figure 15. This information generates rotational Jacobian matrices using Equation (9).

$$J_R = \frac{\partial \omega_n}{\partial \dot{q}} \tag{9}$$

where J_R is the rotational Jacobian, ω_n is the joint angular velocity, and q is the joint angle. Similarly, the translational Jacobian matrix is created using a similar method as the rotational Jacobian matrices. However, it focuses on the transformation of the joint frames. In MATLAB®, the determinant and rank of the matrices associated with the robot's joints are computed for ten interpolated point configurations along the defined path for grasping. The results are shown in Table 4.

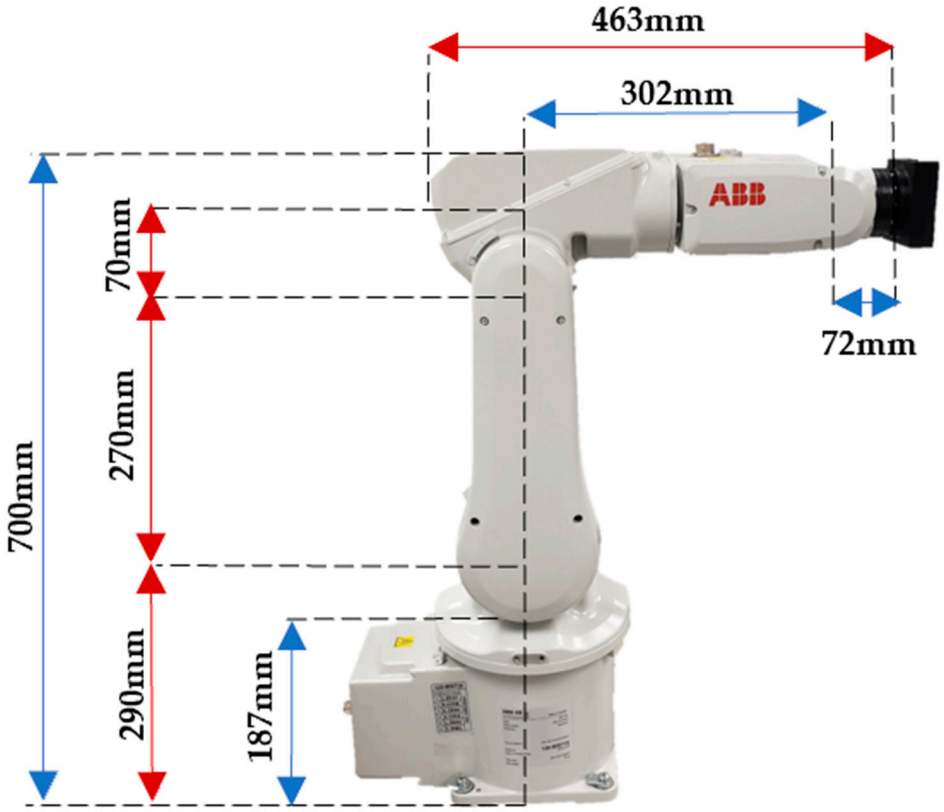

Figure 15. Side view of ABB IRB 120 robotic arm.

The analysis presented in Table 4 confirms that the selected path for the manipulator is devoid of singularities. The robotic arm was programmed based on this path to autonomously execute pick-and-place tasks for a diverse range of objects. Several distinct objects were employed during the grasping test, all of which were successfully grasped by the robot. The successful outcome of the test for grasping various objects with different shapes, sizes, and textures is visually demonstrated in Figure 16. Here, it can be observed that the piston stroke varies for the irregular shape of the object. Especially in Figure 16c, it can be observed that the piston in the vertical direction is more compressed than that of the horizontal ones even though they all had the same motor motion. The objects selected for the test vary in shape, texture, and rigidity. Figure 16a consists of a tomato that is round

and smooth in texture. It is also soft and easily squeezable. In Figure 16b, there is a guava that is a little rougher and harder with unusual shapes. Finally, the object in Figure 16c is a hard plastic bottle with an irregular shape.

Table 4. Determinant and rank of the Jacobian matrices from MATLAB®.

Joint Orientation Angles for All Six Joints q1, q2, q3, q4, q5, q6 (Degrees)	Determinant	Rank
1.98, 3.10, −9.94, −3.12, 56.79, 6.58	−0.0196	6
−26.19, 20.20, −27.12, 17.75, 59.85, −26.26	−0.0198	6
−26.19, 18.38, 6.15, 30.32, 31.47, −43.63	−0.0152	6
−26.19, 22.05, 12.92, 42.40, 43.01, −57.16	−0.0186	6
−26.19, 19.09, 8.08, 32.67, 29.24, −46.35	−0.0143	6
−26.19, 18.49, −17.33, 19.31, 52.86, −29.06	−0.0118	6
15.60, 12.09, −8.52, 15.09, 48.65, 25.56	−0.0199	6
39.66, 35.63, −39.88, −28.25, 64.97, 48.83	−0.0144	6
39.66, 34.93, −6.41, −44.15, 38.01, 73.47	−0.0172	6
39.66, 38.77, −2.22, −52.66, 32.66, 83.87	−0.0159	6

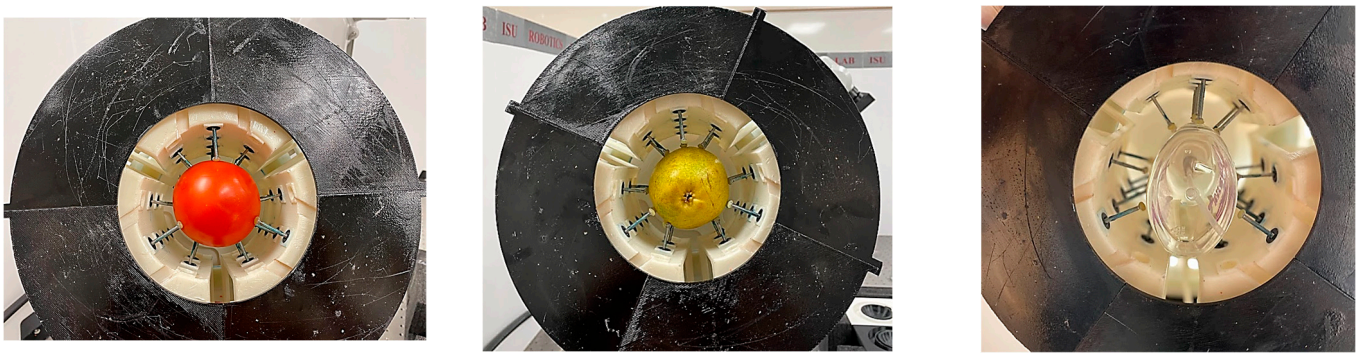

(**a**) (**b**) (**c**)

Figure 16. (**a**) Grasping a tomato; (**b**) grasping a guava; (**c**) grasping a hand sanitizer bottle (all bottom views).

4. Discussions and Conclusions

This paper introduces a novel mechanical gripper design that is specifically tailored for handling objects with diameters ranging from 5 cm to 9 cm. This range is selected based on common fruits and bottles that are typically encountered in food and beverage handling and packaging applications. The gripper's primary purpose is to facilitate the picking and placing of fruits, vegetables, and bottles in grocery stores or warehouses. The design offers ease of actuation, requiring only one actuator and eliminating the need for a closed-loop control system. It features a rotational spring-based grasping mechanism, which can be replaced depending on the weight and texture of the target objects.

By conducting stress analyses and force calculations, the gripper's operational performance was optimized. The analytical studies provided valuable insights, leading to the system meeting its specifications while offering opportunities for enhancements in weight and strength. Through the motion study results, the system could accurately estimate the torque required for achieving the desired range of motion. Likewise, the topology studies conducted on certain components enabled material reduction without compromising their structural strength.

The prototype, which was fabricated using additive manufacturing technology from ABS plastic, underwent successful testing with the intended target objects, which mainly include fruits, vegetables, and other grocery store items. It was observed that the spring and piston's stroke lengths are just as much as it needs and vary depending on the object's shape. To conclude, the research lays out an innovative design as a foundation for vast areas of research and advancement in the material handling and packaging industries.

In future iterations of the gripper, using 6061 aluminum alloy for fabrication will allow for a more compact and smaller form without compromising the strength. Vapor smoothing is recommended for ABS plastic parts to minimize friction. Furthermore, incorporating proper geometric dimensioning and tolerancing (GD&T) techniques can help to eliminate undesired bending moments and high-friction contacts. The electronic control configuration of the gripper, via the robotic arm controller, will contribute to a lighter and more compact design, eliminating the need for a top housing for the motor controller and power. Additionally, the integration of a camera for object detection holds the potential to enable full autonomy in the gripper's operation while exploring its application in space exploration and sample collection. To conclude, the main contributions of this paper are listed as follows:

- Innovative novel gripper design for differently shaped and sized objects;
- Gripper design for soft grasping that also works for rigid objects;
- Able to achieve both force-closure and form-closure grasping;
- Grasping forces from all lateral directions;
- Minimal actuation and simple open-loop control;
- Foundation for future research and sophistication.

Author Contributions: Conceptualization, S.L. and T.D.; methodology, S.L. and T.D.; software, S.L.; validation, S.L. and T.D.; formal analysis, S.L. and T.D.; investigation, S.L.; resources, S.L. and T.D.; data curation, S.L.; writing—original draft preparation, S.L.; writing—review and editing, S.L. and T.D.; visualization, S.L. and T.D.; supervision, T.D.; funding acquisition, S.L. and T.D. All authors have read and agreed to the published version of the manuscript.

Funding: This research received no external funding.

Institutional Review Board Statement: Not applicable.

Informed Consent Statement: Not Applicable.

Data Availability Statement: The data presented in this study are available on request from the corresponding author. The data are not publicly available due to proprietary reasons.

Acknowledgments: The authors extend their kind appreciation to the Department of Mechanical Engineering for facilitating the use of the 3D Printing Laboratory.

Conflicts of Interest: The authors declare no conflict of interest. The funders had no role in the design of the study; in the collection, analysis, or interpretation of data; in the writing of the manuscript; or in the decision to publish the results.

References

1. Anagnoste, S. Robotic Automation Process-The next Major Revolution in Terms of Back Office Operations Improvement. *Proc. Int. Conf. Bus. Excel.* **2017**, *11*, 676–686. [CrossRef]
2. Dixon, J.; Hong, B.; Wu, L. The Robot Revolution: Managerial and Employment Consequences for Firms. *Manag. Sci.* **2021**, *67*, 5586–5605. [CrossRef]
3. Kastan, B. Autonomous Weapons Systems: A Coming Legal "Singularity"? *U Ill. JL Tech. Pol.* **2013**, *2013*, 45.
4. Samadikhoshkho, Z.; Zareinia, K.; Janabi-Sharifi, F. A Brief Review on Robotic Grippers Classifications. In Proceedings of the 2019 IEEE Canadian Conference of Electrical and Computer Engineering (CCECE), Edmonton, AB, Canada, 5–8 May 2019; pp. 1–4.
5. Bicchi, A.; Kumar, V. Robotic Grasping and Contact: A Review. In Proceedings of the 2000 ICRA. Millennium Conference. IEEE International Conference on Robotics and Automation. Symposia Proceedings (Cat. No. 00CH37065), San Francisco, CA, USA, 24–28 April 2000; Volume 1, pp. 348–353.
6. Jacobsen, S.; Iversen, E.; Knutti, D.; Johnson, R.; Biggers, K. Design of the Utah/MIT Dextrous Hand. In Proceedings of the 1986 IEEE International Conference on Robotics and Automation, San Francisco, CA, USA, 7–10 April 1986; Volume 3, pp. 1520–1532.

7. Saito, F.; Fukuda, T.; Arai, F. Swing and Locomotion Control for a Two-Link Brachiation Robot. *IEEE Control Syst. Mag.* **1994**, *14*, 5–12.
8. Lasi, H.; Fettke, P.; Kemper, H.-G.; Feld, T.; Hoffmann, M. Industry 4.0. *Bus. Inf. Syst. Eng.* **2014**, *6*, 239–242. [CrossRef]
9. Reddy, P.V.P.; Suresh, V. A Review on Importance of Universal Gripper in Industrial Robot Applications. *Int. J. Mech. Eng. Robot. Res.* **2013**, *2*, 255–264.
10. Sherwani, F.; Asad, M.M.; Ibrahim, B.S.K.K. Collaborative Robots and Industrial Revolution 4.0 (Ir 4.0). In Proceedings of the 2020 International Conference on Emerging Trends in Smart Technologies (ICETST), Karachi, Pakistan, 26–27 March 2020; pp. 1–5.
11. Dario, P.; Guglielmelli, E.; Allotta, B.; Carrozza, M.C. Robotics for Medical Applications. *IEEE Robot. Autom. Mag.* **1996**, *3*, 44–56. [CrossRef]
12. Kleeberger, K.; Bormann, R.; Kraus, W.; Huber, M.F. A Survey on Learning-Based Robotic Grasping. *Curr. Robot. Rep.* **2020**, *1*, 239–249. [CrossRef]
13. Shorthose, O.; Albini, A.; He, L.; Maiolino, P. Design of a 3D-Printed Soft Robotic Hand with Integrated Distributed Tactile Sensing. *IEEE Robot. Autom. Lett.* **2022**, *7*, 3945–3952. [CrossRef]
14. Wang, Y.; Wu, X.; Mei, D.; Zhu, L.; Chen, J. Flexible Tactile Sensor Array for Distributed Tactile Sensing and Slip Detection in Robotic Hand Grasping. *Sens. Actuators Phys.* **2019**, *297*, 111512. [CrossRef]
15. Deng, Z.; Jonetzko, Y.; Zhang, L.; Zhang, J. Grasping Force Control of Multi-Fingered Robotic Hands through Tactile Sensing for Object Stabilization. *Sensors* **2020**, *20*, 1050. [CrossRef]
16. Ntagios, M.; Nassar, H.; Pullanchiyodan, A.; Navaraj, W.T.; Dahiya, R. Robotic Hands with Intrinsic Tactile Sensing via 3D Printed Soft Pressure Sensors. *Adv. Intell. Syst.* **2020**, *2*, 1900080. [CrossRef]
17. Hao, Y.; Gong, Z.; Xie, Z.; Guan, S.; Yang, X.; Ren, Z.; Wang, T.; Wen, L. Universal Soft Pneumatic Robotic Gripper with Variable Effective Length. In Proceedings of the 2016 35th Chinese Control Conference (CCC), Chengdu, China, 27–29 July 2016; pp. 6109–6114.
18. Song, S.; Drotlef, D.-M.; Paik, J.; Majidi, C.; Sitti, M. Mechanics of a Pressure-Controlled Adhesive Membrane for Soft Robotic Gripping on Curved Surfaces. *Extreme Mech. Lett.* **2019**, *30*, 100485. [CrossRef]
19. Li, H.; Yao, J.; Wei, C.; Zhou, P.; Xu, Y.; Zhao, Y. An Untethered Soft Robotic Gripper with High Payload-to-Weight Ratio. *Mech. Mach. Theory* **2021**, *158*, 104226. [CrossRef]
20. Müller, A.; Aydemir, M.; Glodde, A.; Dietrich, F. Design Approach for Heavy-Duty Soft-Robotic-Gripper. *Procedia CIRP* **2020**, *91*, 301–305. [CrossRef]
21. Song, E.J.; Lee, J.S.; Moon, H.; Choi, H.R.; Koo, J.C. A Multi-Curvature, Variable Stiffness Soft Gripper for Enhanced Grasping Operations. *Actuators* **2021**, *10*, 316. [CrossRef]
22. Wang, D.; Wu, X.; Zhang, J.; Du, Y. A Pneumatic Novel Combined Soft Robotic Gripper with High Load Capacity and Large Grasping Range. *Actuators* **2021**, *11*, 3. [CrossRef]
23. Zheng, Y.; Lei, G.; Zhang, M.; Che, Q. Mechanical Design and Analysis of a Gripper for Non-Cooperative Target Capture in Space. *Adv. Mech. Eng.* **2018**, *10*, 1687814018810649. [CrossRef]
24. Mo, A.; Zhang, W. A Novel Universal Gripper Based on Meshed Pin Array. *Int. J. Adv. Robot. Syst.* **2019**, *16*, 1729881419834781. [CrossRef]
25. Tavakoli, M.; Marques, L.; de Almeida, A.T. Flexirigid, a Novel Two Phase Flexible Gripper. In Proceedings of the 2013 IEEE/RSJ International Conference on Intelligent Robots and Systems, Tokyo, Japan, 3–7 November 2013; pp. 5046–5051.
26. Kang, L.; Kim, S.-H.; Yi, B.-J. Modeling, Design, and Implementation of an Underactuated Gripper with Capability of Grasping Thin Objects. *Machines* **2021**, *9*, 347. [CrossRef]
27. Mo, A.; Fu, H.; Luo, C.; Zhang, W. Concentric Rotation Pin Array Gripper for Universal Grasp. In Proceedings of the 2018 3rd International Conference on Advanced Robotics and Mechatronics (ICARM), Singapore City, Singapore, 18–20 July 2018; pp. 112–117.
28. Thomas, W.; Wegrowski, P.; Lemirick, J.; Deemyad, T. Lightweight Foldable Robotic Arm for Drones. In Proceedings of the 2022 Intermountain Engineering, Technology and Computing (IETC), Orem, UT, USA, 14–15 May 2022; pp. 1–6.
29. PKP245D23A2-R2E/PLE40-40B/P00027, Stepper Motor with Planetary Gearhead (40:1). Oriental Motor USA. Available online: https://catalog.orientalmotor.com/item/42mm-frame-stepper-motors/42mm-pkp-series-2-phase-bipolar-stepper-motors/pkp245d23a2-r2e-ple40-40b-p00027 (accessed on 19 May 2023).
30. Deemyad, T.; Hassanzadeh, N.; Perez-Gracia, A. Coupling Mechanisms for Multi-Fingered Robotic Hands with Skew Axes. In *Mechanism Design for Robotics, Proceedings of the 4th IFToMM Symposium on Mechanism Design for Robotics, Udine, Italy, 11–13 September 2018*; Springer: Berlin/Heidelberg, Germany, 2019; pp. 344–352.
31. Ngoc, T.L.; Nguyen, T.L. Quasi-Physical Modeling of Robot IRB 120 Using Simscape Multibody for Dynamicand Control Simulation. *Turk. J. Electr. Eng. Comput. Sci.* **2020**, *28*, 1949–1964.